ELSEVIER

Biophysical Chemistry 56 (1995) 89–94

Biophysical Chemistry

Site directed spin labeling studies of structure and dynamics in bacteriorhodopsin

Heinz-Jürgen Steinhoff [a,*], Ramin Mollaaghababa [b], Christian Altenbach [c], H. Gobind Khorana [b,*], Wayne L. Hubbell [c,*]

[a] *Institut für Biophysik, Ruhr-Universität Bochum, 44780 Bochum, Germany*

[b] *Departments of Biology and Chemistry, Massachusetts Institute of Technology, Cambridge, MA 02139, USA*

[c] *Jules Stein Eye Institut and Department of Chemistry and Biochemistry, University of California, Los Angeles, CA 90024-7008, USA*

Abstract

Site-directed spin labeling of membrane proteins has been used to determine: (1) the topography of the polypeptide chain with respect to the membrane/solution interface, and (2) the identity and orientation of secondary structure in selected regions. These features are deduced from the collision rates of nitroxide side chains with paramagnetic reagents in solution, and the principles of the method are reviewed with reference to bacteriorhodopsin. The dynamics of the nitroxide side chains relative to the backbone reveal tertiary interactions of the labeled site, and provide a promising means of time-resolving conformational changes. This aspect is illustrated by recent studies of structural changes in bacteriorhodopsin during the photocycle. In these experiments, nitroxide side chains were introduced at residues 72, 101 and 105 after replacement of the original residues by cysteine. Upon flash photolysis, the electron paramagnetic resonance spectrum of a nitroxide at 101, but not those at 72 or 105, is time-dependent. The spectral change develops during the decay of the M-intermediate, and reverses upon return to the ground state. The results suggest a movement of the C–D or E–F interhelical loops during the protonation changes of aspartate 96.

Keywords: Spin labeling; Bacteriorhodopsin photocycle; Protein conformational change; Electron paramagnetic resonance spectroscopy

1. Introduction

Membrane proteins present a difficult problem for structure determination. With a few exceptions, X-ray diffraction data are not available due to unsolved problems of crystallization. Two-dimensional NMR approaches are not applicable due to the lack of high resolution spectra. Site-directed spin labeling (SDSL) is an alternative approach for obtaining structural information. In this technique, spin labels are introduced into the protein at selected positions using cysteine substitution mutagenesis followed by modification of the reactive sulfhydryl with a nitroxide reagent. The collision rates of the nitroxide side chains with paramagnetic reagents in solution provide information on the static structure of the protein, and a brief review of the principles of the technique will be presented below. More recently, the dynamics of spin-labeled side chains have been analyzed in terms of protein tertiary structure. Perhaps the most important outcome of this work has

* Corresponding authors.

0301-4622/95/$09.50
SSDI 0301-4622(95)00019-4

been the resolution of conformational changes in space and time on a millisecond scale. This aspect will be discussed with reference to conformational changes of bacteriorhodopsin (bR) induced by photon absorption [1].

Bacteriorhodopsin is a light driven proton pump in the purple membrane of *Halobacterium salinarium* [2,3]. After photoexcitation of the light-adapted protein, the all-*trans* to 13-*cis* isomerization of the retinal chromophore initiates a cyclic sequence of intermediates that are identified by their optical absorbance maxima and kinetic properties [4]. During this photocycle, a proton is translocated across the cytoplasmic membrane. Bacteriorhodopsin is a unique model system for the study of active transport systems since a model of the bR ground state structure has been derived based on high resolution electron cryo-microscopy [5]. Additional information regarding the structure and function of bR has been obtained from site-directed mutagenesis studies [3,6,7].

2. Structural studies of bacteriorhodopsin based on collision rates between a nitroxide side chain and paramagnetic probes

To introduce a nitroxide side chain into bR, selected residues were mutated to cysteine, and subsequently modified with the sulfhydryl-specific reagent (1-oxyl-2,2,5,5 tetramethylpyrroline-3-methyl)methanethiosulfonate to give the nitroxide side chain designated R1.

The collision frequencies of the attached nitroxides with polar and non-polar paramagnetic reagents

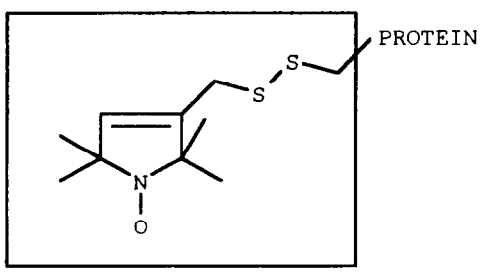

SIDE CHAIN R1

Scheme 1.

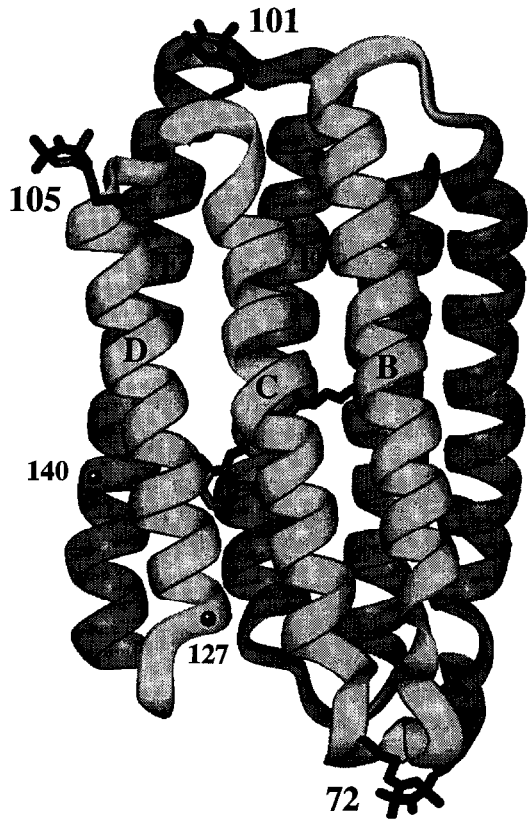

Fig. 1. The structure of the bacteriorhodopsin backbone. The helices are identified as A–G, and spin labels in G72R1, V101R1 and Q105R1 are shown by tube models. Coordinates of the helix segments were obtained from the Brookhaven Protein Data Base. Helix D was shifted by 3 Å towards the cytoplasmic side, as suggested by recent diffraction data. Coordinates for the inter-helical loops were constructed by energy minimization methods. The nitroxide in V101R1 is predicted to be in contact with the E–F interhelical loop.

in solution have been used to determine: (1) the topography of helices C, D and E with respect to the bilayer interface, (2) regions of regular secondary structure, and (3) the orientation of the secondary structure in the protein [8–12]. For example, collision rates of O_2, a hydrophobic probe, with nitroxides in a series of mutants with a single R1 side chain at positions from 129 to 140 show a striking oscillation in the region 131–139 with a period of 3.6, corresponding to the first 2.5 turns of the E helix (Fig. 1) [9]. The orientation of this helical segment in the protein was determined from the phase of the

periodic function: the residues with the lowest collision rate define the helical surface which is oriented towards the interior of the protein, where the solubility of oxygen is low. This helical segment is found to lie within the membrane bilayer based on the low collision rates of the nitroxides with a polar paramagnetic reagent, chromium oxalate (CROX). In contrast, the high values of the collision rate with CROX in the region 127–130 define the water exposed loop region between helices D and E.

3. Structural studies of bR based on analysis of spin label dynamics

The motion of a nitroxide side chain relative to the protein backbone results from rotational isomerizations about internal bonds of the sidechain. Additional constraints on the motion appear to be due to van der Waals interactions with nearby secondary structures, that is, on tertiary interactions [13]. Thus a nitroxide side chain in an isolated helix has little motional restriction relative to one located in a protein interior. Information about the nitroxide mobility, and hence the extent of tertiary interactions, can be extracted from the EPR line shape. For example, consider side chain R1 at positions 105, 109,124 and 127 on the outer surface of the bR D helix, facing the lipid bilayer. Fig. 2 shows transverse sections through the C–D–E helices of bR at the level of each of these residues, along with the corresponding EPR spectra. The spectra at 105 and 109 are similar, both characteristic of rapid thermal motion with a correlation time of a few nanoseconds. On the other hand, the spectra of 124 and 127 reflect significant motional constraints. As illustrated in Fig. 2, this difference can be understood in terms of tertiary interaction of the spin label. At positions 105 and 109, tertiary interactions are absent, and the motion is determined primarily by internal bond isomerization rates. At 124 and 127, the nitroxide directly interacts with helices E and C, respectively, giving rise to additional constraints on the motion. It is easy to appreciate that any relative movement of these helices would modulate the tertiary interactions of the nitroxide and produce time-dependent spectral changes. This provides a powerful means of investigating conformational changes in proteins, and in the

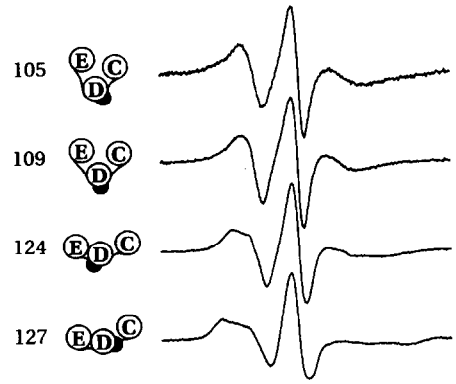

Fig. 2. The effect of tertiary interactions on the EPR spectra of nitroxide side chain R1 in bR. Left column: slices through the C–D–E helical region of bacteriorhodopsin. Each slice is taken in a plane containing the indicated residue, and the dot identifies the position of the beta carbon atom of the R1 side chain. Right column: EPR spectra for the indicated mutants.

remainder of the paper we review the time-resolved EPR detection of structural changes in bR during the photocycle [1].

4. Studies of conformational changes in bR during the photocycle using spin-labeled mutants

The sequence of intermediates in the photocycle of bR is associated with significant conformational changes in the protein. Difference density projection maps obtained by neutron and electron diffraction studies reveal significant changes near helices G and B and between helix E and F [14], [15]. Time-resolved X-ray diffraction studies on a bR mutant with a slow photocycle show that structural changes occur during the transition from bR_{570} to the M_{412} intermediate, and recover during the N_{560} to bR_{570} transition [16]. Time-resolved FTIR experiments reveal that the main structural changes of the protein backbone, indicated by amide I and amide II difference bands, take place during the M_{412} to N_{560} transition [17,18].

As an alternative approach, the technique of SDSL provides both real-time resolution and specific localization of structural changes. To study structural changes in bR during the photocycle, we have em-

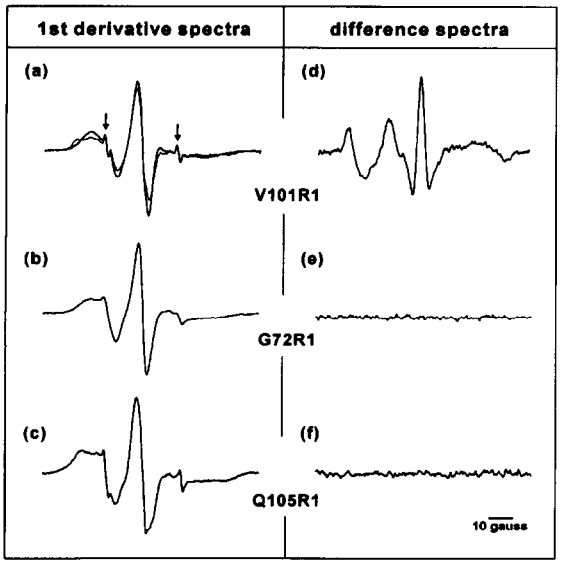

Fig. 3. First derivative EPR spectra of V101R1, Q105R1 and G72R1 are shown by the bold traces in (a)–(c). The difference EPR spectra due to photoexcitation, recorded as described in the text, are shown in (d)–(f). A spectral change is observed only for V101R1. The thin trace in (a) shows the EPR spectrum as it appears 30 ms after the flash. This spectrum was calculated as the sum of the difference spectrum (d) and the ground state spectrum (bold trace in (a)).

ployed bR mutants G72R1 [1], V101R1 and Q105R1. For all energetically reasonable conformations of the spin label, the nitroxide group of the label bound to V101R1 on the cytoplasmic side of the molecule is located close to the E–F loop (Fig. 1). The nitroxide ring bound to Q105R1 points into the opposite direction towards the B helix of an adjacent bR molecule in the protein lattice trimer. The interactions of the nitroxide in G72R1 cannot be determined due to uncertainties in the conformation of the relatively long B–C interhelical loop.

The EPR spectra of G72R1, V101R1 and Q105R1 are shown in Fig. 3a–c. The nitroxides at G72R1 and V101R1 show a similar degree of intermediate immobilization due to tertiary interaction, while the nitroxide in Q105R1 is more immobilized. Changes of the EPR spectra due to photoexcitation were monitored directly by phase sensitive detection of the EPR spectrometer signal referenced to a 0.5 Hz actinic xenon flash. This detection scheme gives directly the difference spectra between the bR ground state and excited state conformations (Fig. 3d–f). The difference spectra show significant changes in the mobility of the spin label in V101R1 subsequent to photoexcitation. The spin label mobility is transiently decreased as can be deduced from the changes in the low and high field line shapes. The EPR spectrum of V101R1 30 milliseconds after the flash is shown in Fig. 3a (light trace), and clearly shows the higher degree of immobilization in the excited state of the protein. The conformational change of the protein causing this signal change is apparently not global since no spectral changes are detected at positions 72 and 105.

To determine the intermediate of the photocycle that corresponds to the observed motion, the time dependence of the EPR signal was followed after an actinic light-flash of 150 μs duration at fixed magnetic field. The results are shown in Fig. 4 for V101R1, together with the optical transients of the spin-labeled sample at 412 nm and 570 nm. The conformational changes responsible for the EPR spectral change appear during the decay of the M_{412} intermediate and reverse with the recovery of the bR_{570} ground state. Hence, the observed structural change can be assigned to an intermediate lying between M_{412} and bR_{570}. This is consistent with results from time resolved FTIR experiments [17,19] and time resolved X-ray diffraction studies [16].

The replacement of the natural amino acids at positions 101, 105 or 72 by a cysteine does not shift the absorption band of the bR ground state and does not significantly affect the photocycle kinetics (U. Alexiev, R. Mollaaghababa, H.G. Khorana, M.P. Heyn, unpublished). After spin labeling, the photocycles of G72R1 and Q105R1 remain unaffected, while the decay times of M_{412} and the recovery of bR_{570} in V101R1 are increased by a factor of 10. The use of a methanethiosulfonate nitroxide derivative with the side chain increased in length by 3 Å shows a smaller effect on the photocycle time [1]. In this case, the M_{412} decay is slowed down by only a factor of two compared to the wild type protein, and the magnitude of the EPR spectral changes subse-

[1] Mutant proteins will be identified with the original side chain, the position number, and the substituted side chain. Thus G72R1 is a mutant in which glycine 72 was mutated to cysteine and subsequently modified to produce spin label side chain R1.

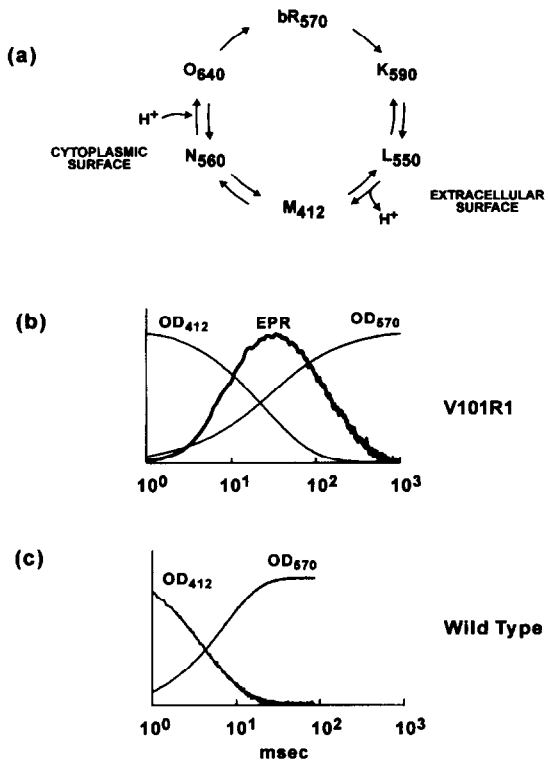

Fig. 4. (a) The photocycle of bacteriorhodopsin. Back reactions have been added to the original scheme of Lozier et al. [4], and only one M-intermediate is shown, although at least two distinct forms have been proposed [23,24]. (b) Optical absorbance and EPR transients following a light flash for spin labeled mutant V101R1. For the EPR transients, the magnetic field was fixed at the maximum of the difference signal. The optical absorbances at 412 nm and 570 nm monitor the M-intermediate and the ground state, respectively. The conformational transitions responsible for the EPR spectral changes appear with the decay of the M-intermediate and reverse with the recovery of the bR ground state. For comparison, the optical absorbance transients for the wild type protein are shown in (c).

quent to photoexcitation is reduced. This is expected since the increase in distance between the nitroxide moiety and the protein backbone reduces their interaction. Therefore the trade-off for a smaller effect on the photocycle kinetics is a lower signal-to-noise ratio for the EPR transient signals.

What kind of conformational change could account for the observed EPR spectral change? The structural change is detected at the cytoplasmic surface of the bacteriorhodopsin molecule in C–D interhelical loop (Fig. 1). The E–F interhelical loop is in close apposition to the nitroxide attached to site 101. Thus, motion of any of the helices E, F, C or D at the cytoplasmic surface could influence the nitroxide mobility and therefore account for the data. However, the spin labels bound at positions 105 and 72 do not sense any changes upon photoexcitation. Therefore, structural rearrangements of the cytoplasmic side of helix D and of the extracellular side of helix C during the latter half of the photocycle are considered less likely.

The EPR data reveals that the conformations of M_{412} and the bR_{570} ground state are similar in the region of the nitroxides, and that the structural changes take place during the decay of M_{412}. However, diffraction data reveals structural changes already at M_{412} which relax during the recovery of the bR_{570} ground state [15,16,20]. The reason for this may be the different spatial resolution of the two techniques. While the diffraction difference density maps show a projection of all changes along a helix, the SDSL technique reveals only conformational rearrangements near the nitroxide. Thus the structural changes revealed by diffraction experiments and assigned to the M_{412} intermediate may be distant from site 101. Alternatively, it is possible that different M-like conformations have been analyzed, since different conditions for sample preparation and temperatures were used in the different techniques.

In summary, a localized structural change is detected in the vicinity of V101, that occurs during the decay of the M_{412} intermediate and relaxes during the recovery to the ground state. The spin labeled residue in V101R1 is only five residues apart from aspartate 96, which transfers a proton to the Schiffs base during M_{412} decay [21], and is re-protonated from solution during the decay of N_{560} [18,22]. The EPR signals changes thus may reflect the structural changes near V101 due to protonation changes of aspartate 96.

Acknowledgements

Supported by a Max Kade Foundation Fellowship (H.-J.S.), NIH grants GM28289 and AI11479 (H.G.K.) and EY05216 (W.L.H.) and the Jules Stein Professor endowment (W.L.H.).

References

[1] H.-J. Steinhoff, R. Mollaaghababa, K. Hideg, M. Krebs, H.G. Khorana and Wayne L. Hubbell, Science, 266 (1994) 105.
[2] W. Stoeckenius and R.A. Bogomolni, Ann. Rev. Biochem., 51 (1982) 587.
[3] H.G. Khorana, J. Biol. Chem., 263 (1988) 7439.
[4] R.H. Lozier, R.A. Bogomolni and W. Stoeckenius, Biophys. J., 15 (1975) 955.
[5] R. Henderson, J.M. Baldwin, T.A. Ceska, F. Zemlin and E. Beckmann, J. Mol. Biol., 213 (1990) 899.
[6] R. Needleman, M. Chang, B. Ni, G. Varo, J. Fornes, S.H. White and J.K. Lanyi, J. Biol. Chem., 266 (1991) 11478.
[7] M.P. Krebs, R. Mollaaghababa and H.G. Khorana, Proc. Natl. Acad. Sci. USA, 90 (1993) 1987.
[8] C. Altenbach, S.L. Flitsch, H.G. Khorana and W.L. Hubbell, Biochemistry, 28 (1989) 7806.
[9] C. Altenbach, T. Marti, H.G. Khorana and W.L. Hubbell, Science, 248 (1990) 1088.
[10] C. Altenbach, D. Greenhalgh, H.G. Khorana and W.L. Hubbell, Proc. Natl. Acad. Sci. USA, 91 (1994) 1667.
[11] C. Altenbach, H.-J. Steinhoff, D.A. Greenhalgh, H.G. Khorana and W.L. Hubbell, Biophys. J., 65a (1994) 44.
[12] D. Greenhalgh, C. Altenbach, W.L. Hubbell and H.G. Khorana, Proc. Natl. Acad. Sci. USA, 88 (1991) 8626.
[13] W.L. Hubbell and C. Altenbach, Curr. Opinions Struct. Biol., 4 (1994) 566.
[14] N.A. Dencher, D. Dresselhaus, G. Zaccai and G. Büldt, Proc. Natl. Acad. Sci USA, 86 (1989) 7876.
[15] S. Subramanian, M. Gerstein, D. Oesterhelt and R. Henderson, EMBO J., 2 (1993) 1.
[16] M.H.J. Koch, N.A. Dencher, D. Oesterhelt, H.-J. Ploehn, G. Rapp, G. Büldt, EMBO J., 10 (1991) 521.
[17] G. Souvignier and K. Gerwert, Biophys. J., 63 (1992) 1393.
[18] K.J. Rothschild, T. Marti, S. Sonar, Y.W. He, P. Rath, W. Fischer, H.G. Khorana, J. Biol. Chem., 268 (1993) 27046.
[19] J.-M. Pfefferle, A. Maeda, J. Sasaki and T. Yoshizawa, Biochemistry, 30 (1991) 6548
[20] M. Nakasako, M. Kataoka, Y. Amemiya and F. Tokunaga, FEBS Lett., 292 (1991) 73
[21] H. Otto, T., Marti, M. Holtz, T. Mogi, M. Lindau, H.G. Khorana and M.P. Heyn, Proc. Natl. Acad. Sci. USA, 86 (1989) 9228.
[22] K. Gerwert, G. Sougvignier and B. Hess, Proc. Natl. Acad. Sci. USA, 87 (1990) 9774.
[23] G. Váró and J.K. Lanyi, Biochemistry, 30 (1991) 5008.
[24] G. Váró and J.K. Lanyi, Biochemistry, 30 (1991) 5016.